July, 1985]   © 1985 The Chemical Society of Japan   Bull. Chem. Soc. Jpn., 58, 2043—2050 (1985)   2043

Formaldehyde Electro-oxidation on Copper Metal and Copper-based Amorphous Alloys in Alkaline Media

Ken-ichi Machida and Michio Enyo*
Research Institute for Catalysis, Hokkaido University, Sapporo 060

(Received March 6, 1985)

Copper metal and copper-based amorphous alloys, a-$Cu_{35}Ti_{65}$ and a-$Cu_{33}Zr_{67}$, exhibit a very high and stable activity for the anodic HCHO oxidation in aqueous NaOH and Na_2CO_3. The oxidation current was already observable at electrode potentials as low as 0.1 V (RHE) and, in particular, the HF-treated amorphous alloys gave high current densities around 40 mA cm^{-2} (apparent) at 0.2 V. Kinetic data, roughly first order both in HCHO and OH^- concentration, are in favour of the mechanism in which the oxidation proceeds *via* hydroxymethanolate ion ($HOCH_2O^-$) formed from HCHO and OH^-, producing $HCOO^-$ and H_2: This ion is readily oxidized on the copper metal or copper-based amorphous alloy electrodes. The Tafel slope was in general agreement with the reaction mechanism assuming a rate-determining one-electron transfer step.

Fuel cells which employ organic fuels such as methanol or its derivatives are strongly demanded, especially for uses as small scale transportable electric power sources with improved conveniences in storage and handling of the fuel as compared with hydrogen. A number of investigations on this subject have been carried out about two decades ago,[1-3] but fuel cells of this type which are economically comparable with other electric power sources have not yet been developed. A major difficulty involved in some carbonaceous fuel cells is due to sluggish rate of electro-oxidation of the fuels. Hence, a breakthrough which must be accomplished before developing such fuel cells is concerned with the fabrication of electrodes having high electrocatalytic activity towards the oxidation.

A series of precious metals generally possess high activity compared with other metals for the electro-oxidation of these fuels and most investigations carried out up to this date have been concentrated on them.[2] At the present stage, it appears that the following two directions may be sought for in order to attain fuel cells which are economically more feasible: Thus, (a) the electrocatalytic activity per unit loading of the precious metal should be improved so that its amount of use may be reduced or (b) nonprecious metal electrodes with high electrocatalytic acivity for organic fuels should be developed.

As electrode materials other than precious metals, tungsten carbides[2c] and molybdenum oxides[3c] have been noted, and some workers[4,5] have lately reported that these electrodes have excellent characteristics for the electro-oxidation of methanol or its derivatives. Among methanol derivatives, formaldehyde can readily be electro-oxidized on some nonprecious metals: The present authors have recently reported that a series of IB metals catalyze the anodic HCHO oxidation[6] in alkaline media and suggested a possible use of Cu metal or Cu-based amorphous alloys as electrocatalysts.[6c] In this paper, some further details of the anodic oxidation characteristics in both aqueous NaOH and Na_2CO_3 media are presented and then the reaction mechanism is presented.

Most amorphous alloys prepared by the rapid quench technique generally have a high strength to mechanical stresses. They are also often corrosion resistant because they are essentially in the form of homogeneous solid solutions of the alloying metals and contain no lattice defects, *e.g.* dislocation, grain boundary, *etc.* Their uses as catalysts or electrocatalysts have drawn attentions during the last several years. In the field of electrocatalysis, Kawashima and Hashimoto[7] reported electro-oxidation of methanol and its derivatives in alkaline solutions on a series of Pd-based amorphous alloys such as a-$Pd_{61}Pt_{20}P_{19}$. A number of amorphous Cu–Ti and Cu–Zr alloy specimens with compositions between 30 and 70 wt% Cu have been prepared and the hydrogen absorbability has been studied.[8] The hydrogen evolution reaction property and surface characteristics of HF-treated Cu-based amorphous alloy specimens have been reported in our previous paper.[9]

Experimental

Preparation of Electrodes. The Cu electrodes were prepared from an ordinary Cu plate (0.3 mm in thickness, 99.5% purity) in a rectangular form of 10×5 mm and their surface was etched with dilute nitric acid prior to the electrochemical measurements. The electrodes of Cu-based amorphous alloys were made from alloy ribbons (0.5—1.0 mm wide and *ca.* 20 μm in thickness)[†] and made porous by treatment with aq HF as described elsewhere.[9] The electrodes were clipped or spot-welded on Ta lead wires which were sealed in Pyrex glass tubings.

Roughness Factor. The roughness factor (*RF*) of the electrodes was evaluated from the double layer capacitance

---

[†] Some of these samples were provided by Prof. K. Suzuki and Dr. K. Kai of Tohoku University, to whom our thanks are due.

data measured by a galvanostatic transient method (time scale=1—5 m s) and the assumed value of 18 μF cm^{-2} (true).

Electrochemical Measurements. The cyclic voltammogram and steady-state polarization measurements were carried out in 0.03—3.0 M (M=mol dm^{-3}) NaOH or 0.5 M Na_2CO_3 solutions, which contain various amounts of HCHO (0.003—1.0 M), under a stream of purified Ar gas. The formaldehyde used (GR grade, Nakarai Chemicals, Tokyo) contained 7 wt% CH_3OH. A Ag/AgCl and a pt-Pt RHE were used as reference electrodes, but all the potential values quoted in this report are given on the RHE scale. Details of the cell and other experimental procedures were described previously.[6)]

XPS Measurements. Surface analysis of the amorphous Cu–Ti and Cu–Zr alloys was performed using an ESCA apparatus (VG-III) with Mg *Kα* radiation. The binding energy values recorded were calibrated using the $4f_{7/2}$ signal (83.8 eV) from a gold plate which was employed as an internal standard.

Results and Discussion

In NaOH Solutions. The electrocatalytic activity of Cu metal electrodes for the electro-oxidation of HCHO was very high. The rest (open circuit) potential of Cu metal and Cu-based amorphous alloy electrodes was usually observed to be around −50 mV (RHE). Although this value is much more positive than the theoretical oxidation potential of HCHO (−0.22 V *vs.* RHE), it is the most negative potential observed among analogous systems employing various carbonaceous fuels.

Figure 1 shows typical cyclic voltammograms obtained on a Cu plate in 1 M NaOH containing various amounts of HCHO. Even with HCHO of very low concentration (10^{-2} M), the oxidation current was quite significant and it became already noticeable at potentials around 0.1 V. The hysteresis on the cyclic voltammograms, which is very often observed in the electro-oxidation of carbonaceous fuels such as methanol, was small or almost absent in this case under the polarization between 0 and 0.5 V. The decrease of the current density above about 0.4 V observed in 0.01 M HCHO solution may perhaps be attributed, under the short HCHO supply conditions, to the formation of oxide (*e.g.* Cu_2O) on the Cu surface at that potential, which may give rise to the lowering of the electrocatalytic activity. Such a deactivation never took place in solution containing higher amounts of HCHO.

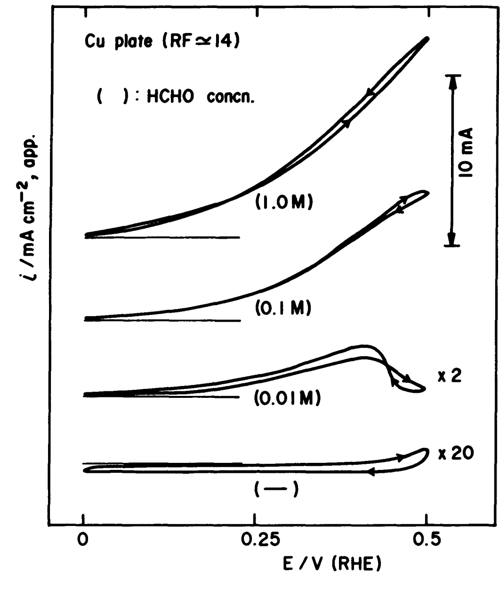

Fig. 1. Typical cyclic voltammograms observed on a Cu plate in 1 M NaOH containing 0.01—1.0 M HCHO at 303 K. Potential sweep rate: 10 mV s^{-1}.

In a previous paper,[9)] we have reported that Cu-rich porous layers formed by the treatment with aq HF on the surface of the amorphous Cu–Ti and Cu–Zr alloys show a high electrocatalytic activity for the hydrogen evolution reaction as compared with usual smooth Cu electrodes. Similarly, very high HCHO electro-oxidation currents were observed on the HF-treated amorphous Cu–Ti and Cu–Zr alloy electrodes and, among them, the latter alloy showed more active and hence advantageous electrocatalytic characteristics than the former one. Meanwhile, the HCHO oxidation current on the untreated Cu-based amorphous alloys was very small: This must be due to the existence of inert oxide films, *i.e.* TiO_2 or ZrO_2, covering their surface.

Figure 2 shows cyclic voltammograms observed on the HF-treated amorphous Cu–Ti and Cu–Zr alloys with various *RF* values (given in the parentheses). On the Cu–Ti alloy electrodes, the current-voltage curves have maxima with a peak around 0.35 V in a similar manner as that of the Cu plate at the concentration of 0.01 M HCHO (see Fig 1). On the other hand, the voltammograms on the Cu–Zr alloys have no such maxima and increase monotonously with the potential sweep. In addition, the hysteresis on the voltammograms of these specimens is considerably smaller, and the catalytic activity of the electrodes with analogous *RF* values is much higher, as compared with that of the amorphous Cu–Ti alloy. These observations may suggest a difference in the surface characteristics of the porous Cu layers formed from the Cu–Ti and Cu–Zr alloys by the HF-treatments.

The surface of the Cu-based amorphous alloys was made porous by dissolving the alloy component Ti and Zr out of the alloy matrices with aq HF: It has been observed from SEM pictures that the surface indeed has a porous structure.[9)] Nevertheless, the Cu-rich porous layers formed in this way contained a noticeable amount of Ti or Zr residue, as demonstrated in the XPS patterns of the Cu–Ti and Cu–Zr alloys which were observed before and after the HF-

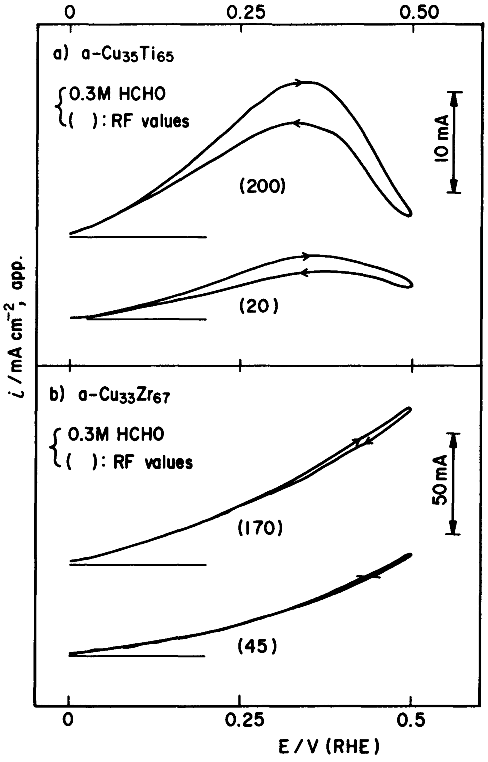

Fig. 2. Cyclic voltammograms observed on the Cu-based amorphous alloy electrodes with several *RF* values in 1 M NaOH containing 0.3 M HCHO at 303 K. Potential sweep rate: 10 mV s^{-1}.

treatment (shown in Fig. 3).

On both the untreated and HF-treated specimens, spectra derived from strong Ti_{2p} and Zr_{3d} electrons have signals at the binding energy regions of 459—465 and 183—186 eV, respectively: These peak positions agree with those of the titanium of TiO_2 and the zirconium of ZrO_2, respectively. The O_{1s} signals consist of two bands peaking at about 530.6 and 532.7 eV which can respectively be assigned to the oxygens of oxides and hydroxyl groups. The Cu_{2p} signals are attributable to the 2p electrons of the metallic copper and/or Cu_2O. After the HF-treatments, however, the spectrum intensities from Cu_{2p} electrons are considerably increased whereas those of Ti_{2p} or Zr_{3d} electrons decreased.

It can be seen from Fig. 3 that the amounts of the Ti and Zr residue in the resulting Cu-rich layers on the HF-treated amorphous Cu–Ti and Cu–Zr alloys nevertheless differ considerably from each other: The amorphous Cu–Zr alloy gives relatively strong Zr_{3d} signals even after the HF-treatment while this was not the case for Ti in the amorphous Cu–Ti alloys. Thus, the Cu-rich layers formed on the amorphous Cu–Zr alloy still contain an appreciable amount of Zr, and the improved electrocatalytic activity of the amorphous Cu–Zr alloy may be due to this Zr residue. On the other hand, Ti was almost completely lost from the surface of the Cu–Ti alloy and this was probably the reason why the characteristics of the Cu-rich layers on this alloy was rather similar to those of usual Cu plates.

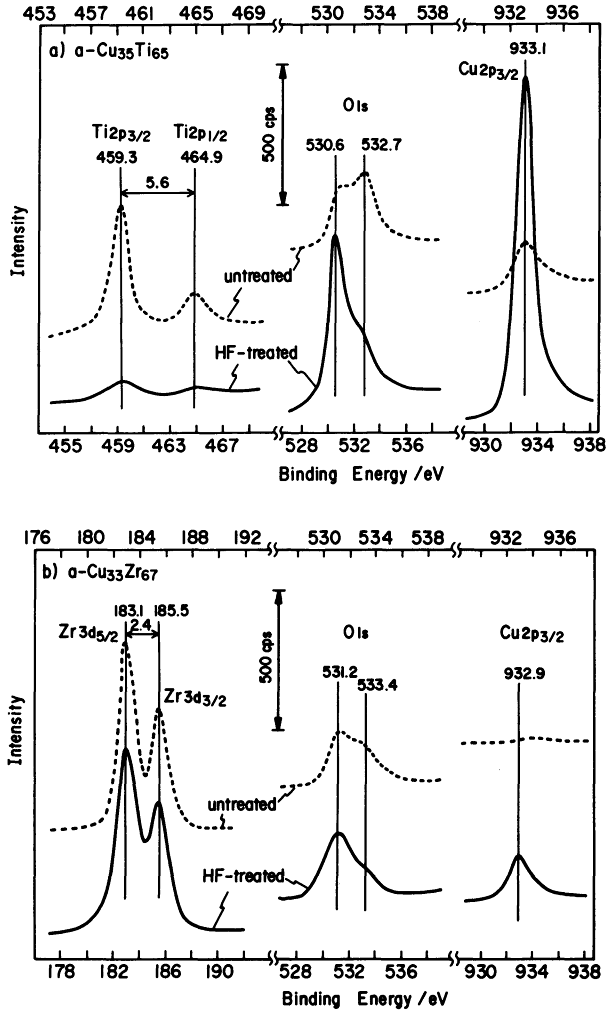

Fig. 3. XPS patterns of the Ti_{2p} (or Zr_{3d}), O_{1s}, and Cu_{2p} electrons on (a) a-$Cu_{35}Ti_{65}$ and (b) a-$Cu_{33}Zr_{67}$ alloys before (broken-lines) and after (solid-lines) the treatment with aq HF.

The difference between Cu–Ti and Cu–Zr alloys is again demonstrated in the relationship between the oxidation current density and *RF* values, as shown in Fig. 4 together with results obtained on the Cu metal electrodes. The current increased initially in a proportional way with the *RF* values and the highest value reached on the amorphous Cu–Zr alloy at 0.2 V was around 40 mA cm^{-2}. An analogous shape was also obtained on the Cu–Ti alloy. Although the data were rather erratic, it could be seen in general that the current density was much lower than that on the Cu–Zr alloy. In the region of still higher *RF* values, the current had a tendency to reach a saturation value. This might indicate that not all the surface area of the porous alloy electrodes was any longer used effectively in the oxidation of HCHO: The curve suggests that the electrode with the *RF* value above 100 is quite satisfactory for the HCHO electro-oxidation.

A kind of "induction period" was seen in Fig. 4 on electrodes with low *RF* values: These were obtained on the electrode without any extensive treatment of the surface. This might indicate that the amorphous alloys became electrocatalytically active only after a significant amount of the inert oxide films (TiO_2 or ZrO_2) was lost from the surface so that their surface became sufficiently rich in Cu.

The electrocatalytic activity was very stable: Large current density values were obtained even after a prolonged time of the steady-state polarization on those electrodes, particularly on the HF-treated amorphous alloys with the porous Cu-rich layers formed on the surfaces. Figure 5 shows the stability of the electrocatalytic activity of Cu metal and Cu-based amorphous alloys at the initial period of the steady state polarization at 0.2 V. No steep decay in the anodic current density, such as those frequently observed in the methanol oxidation on platinum electrodes was recorded. In a long period (several days) polarization, however, a further amount of formaldehyde must be added to the electrolyte in order to maintain the stable current density outputs. This indicated that HCHO would have been decomposed to methanol and formate by the Cannizzaro disproportionation reaction in alkaline media.

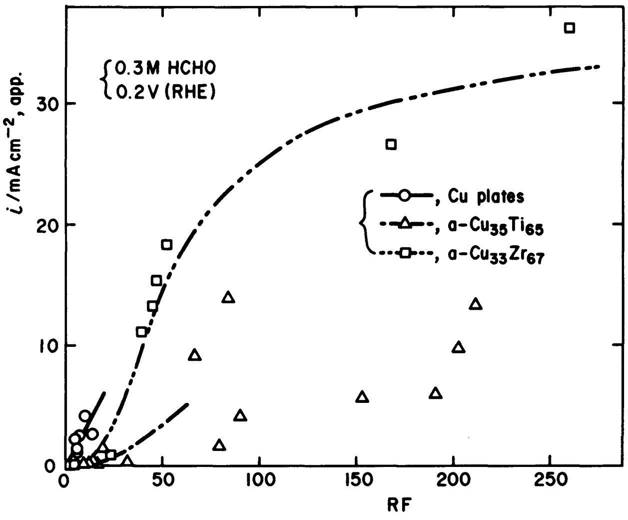

Fig. 4. *RF* value dependences of the anodic current density i on Cu metal and Cu-based amorphous alloy electrodes in 1 M NaOH containing 0.3 M HCHO at 303 K. The i values are read at 0.2 V on the cyclic voltammograms obtained with the potential sweep range of 0—0.5 V and the sweep rate of 10 mV s^{-1}.

In Na_2CO_3 Solutions. If the oxidation of HCHO in alkaline solutions such a NaOH and KOH is complete, yielding CO_2 (and H_2O), the alkali would readily take up CO_2 and form carbonate and then hydrogencarbonate. This means that the cell reaction consumes the alkali metal hydroxide rather like a part of fuels. It is then much more advantageous if the electro-oxidation of HCHO takes place with a reasonable rate in Na_2CO_3 solution. In this case, the fuel cell may be operated at relatively high temperatures so that the hydrogencarbonate is decomposed back to carbonate.

Figure 6 shows typical cyclic voltammograms observed on a Cu plate in 0.5 M Na_2CO_3 solution. As same as those obtained in NaOH solutions, the anodic oxidation current of HCHO was clearly observed at potentials lower than 0.1 V and the rest potential was again negative on the RHE scale. The hysteresis of their voltammograms are very small. The electrocatalytic activity of the Cu-based amor-

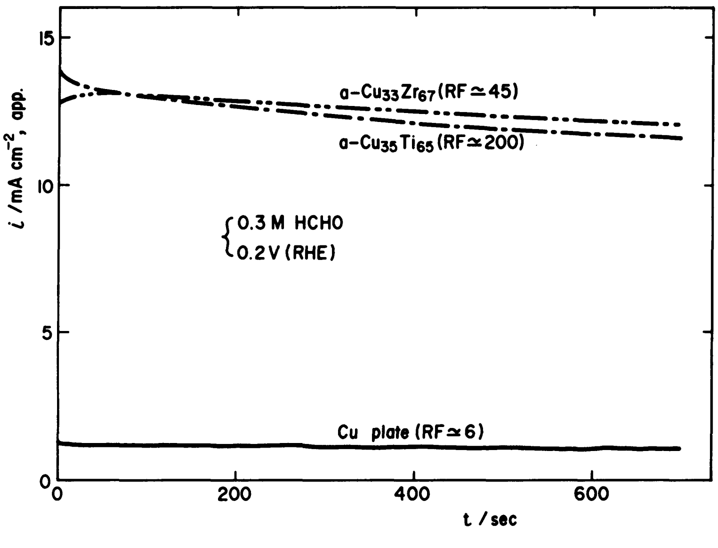

Fig. 5. Time dependences of the anodic current density i under the steady-state polarization at 0.2 V on Cu metal and Cu-based amorphous alloy electrodes in 1 M NaOH containing 0.3 M HCHO at 303 K.

phous alloys was much higher than that of the Cu metal electrodes. Nevertheless, their anodic current outputs were about one order of magnitude smaller than those obtained in NaOH solutions.

The anodic current outputs are maintained practically at constant values for a long period over several days: The Cu-based amorphous alloys with *RF* value of 110—120 constantly give the current density around 3 mA cm^{-2} (see Fig. 7), and thus these alloys are again good candidates for the electrode materials in this type of formaldehyde fuel cells.

Reaction Mechanism. Tafel plots of the anodic polarization currents on the Cu metal and Cu-based amorphous alloys are shown in Fig. 8. It is seen as mentioned already that all the rest potentials are negative to RHE and the catalytic activity is very high. The slopes of the linear portions in their Tafel plots are not much different from the ordinary behaviours of one-electron transfer kinetics, although the behaviour of the amorphous Cu-Ti alloy electrode is somewhat different from the others. The slope values would indicate that the oxidation takes place by a mechanism involving a rate-determining one-electron transfer step.

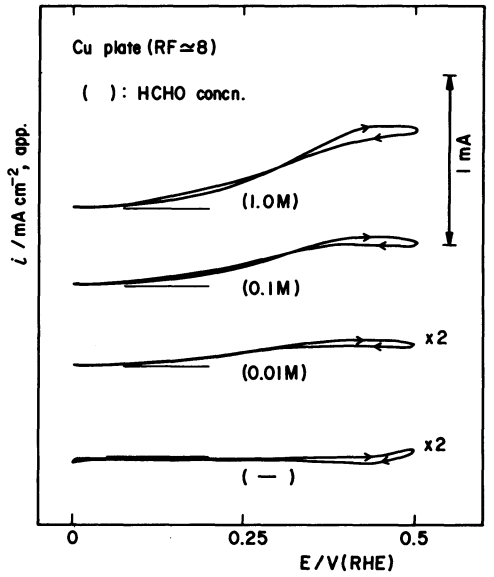

Fig. 6. Typical cyclic voltammograms observed on a Cu plate in 0.5 M Na_2CO_3 (pH=11.5) containing 0.01—1.0 M HCHO at 303 K. Potential sweep rate: 10 mV s^{-1}.

Meanwhile, evolution of hydrogen during the reaction, in spite of more positive electrode potentials than that of the RHE were involved, was reported by some investigators in experiments which are connected with the electroless plating[10c,d] of metals such as Cu: This was also confirmed in the present work.

The number of electrons involved in the electro-oxidation was evaluated from the quantity of electricity required when a given amount of HCHO was completely electro-oxidized at a constant electrode potential. Figure 9 shows a coulometric curve of the anodic HCHO oxidation on a Cu plate electrode. The number obtained was 0.97 equivalents mol^{-1} during the electrolysis at 0.23 V in 1 M NaOH solution. This observation indicates that the reaction is a partial oxidation to $HCOO^-$, along with a co-production of hydrogen.

In Fig. 10 is shown a relation between the anodic current density on the Cu metal electrode and pH of NaOH solutions, 0.03—3.0 M, which contain 0.3 M HCHO. At the lower pH region, the curve obtained was asymptotic to the line with the slope of unity (dashed line in figure): The oxidation reaction may thus be judged to be first order in OH^- in low NaOH

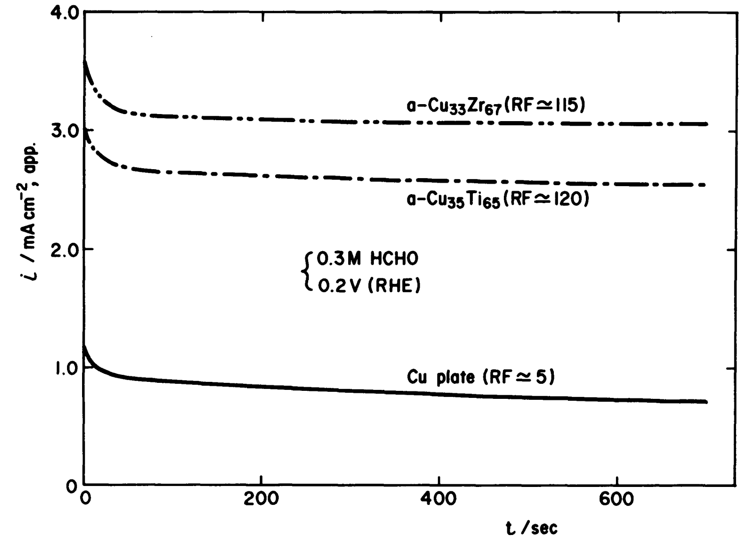

Fig. 7. Time dependences of the anodic current density i under the steady-state polarization at 0.2 V on Cu metal and Cu-based amorphous alloy electrodes in 1 M NaOH containing 0.3 M HCHO at 303 K.

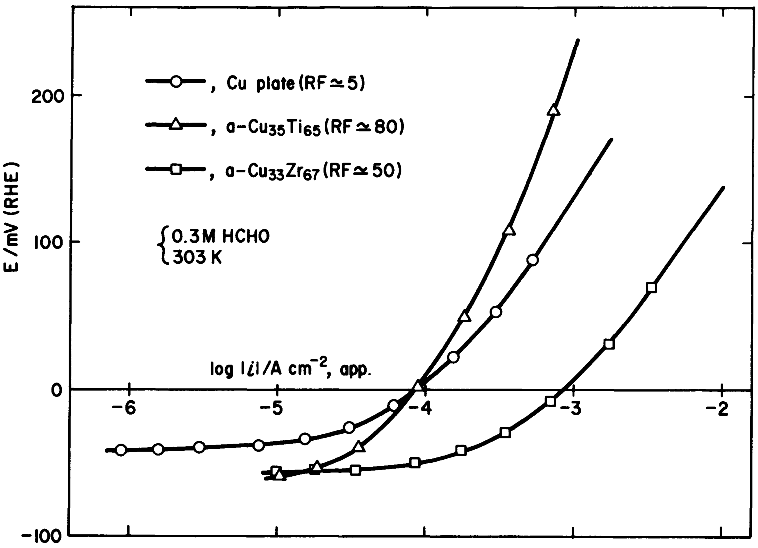

Fig. 8. Anodic polarization behaviors of Cu metal and Cu-based amorphous alloy electrodes in 1 M NaOH containing 0.3 M HCOH at 303 K.

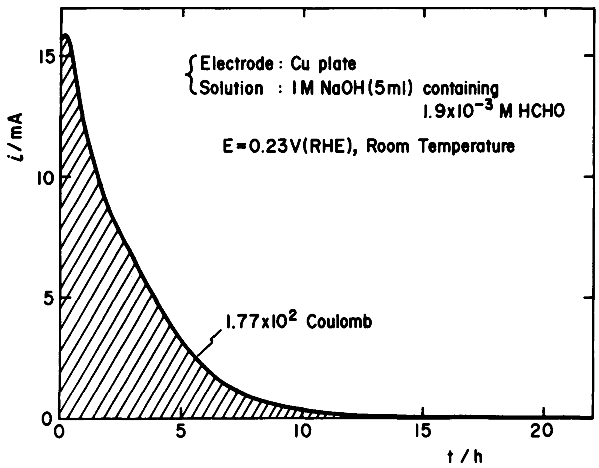

Fig. 9. A coulometric curve of the anodic formaldehyde oxidation on a Cu plate.

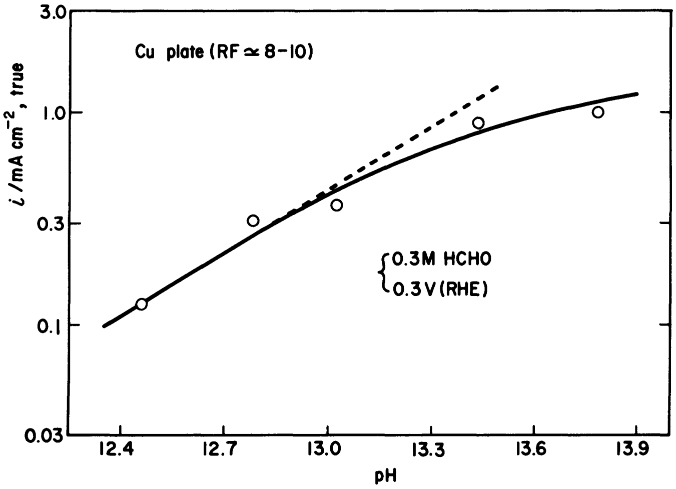

Fig. 10. Anodic current density i vs. pH observed on Cu plates in 0.03—3.0 M NaOH solutions containing 0.3 M HCHO at 303 K.

concentration range.

The dependence of the oxidation rate on the HCHO concentration on the Cu metal electrode with a fixed NaOH concentration is shown by open circles in Fig. 11. The log-log plot again yields a smooth bending curve, but it has a general tendency to approach a line with the slope of unity at low concentrations, in a similar manner as in Fig. 10. These observations, *i.e.* the oxidation rate increases with increase both in HCHO or OH^-, are in harmony with the mechanism proposed in the literature[10)] that hydroxymethanolate (methyleneglycol) ion, $HOCH_2O^-$, is formed from HCHO in aqueous alkaline solutions, and the anodic HCHO oxidation proceeds *via* this ion.

This reaction scheme means that pH of the alkaline solution should decrease by the addition of HCHO or the equilibrium constant for the formation of $HOCH_2O^-$ can be evaluated from the pH change. In Table 1, the pH values of NaOH solutions observed before and after the addition of the equimolar amounts of HCHO, and the K values thus evaluated are summarized. As an average, K=4.7 M^{-1} was obtained, although the K value at high NaOH concentration (0.298 M) was too high as compared with the other values.

Also presented in Fig. 11 (filled circles) is the relation between the oxidation current and the $HOCH_2O^-$ concentration evaluated from the reactant concentrations and the K value obtained above. It may be seen that the reaction is essentially of the first order with respect to $HOCH_2O^-$ at low concentrations. The decrease of the reaction order in the higher concentration region may require more information

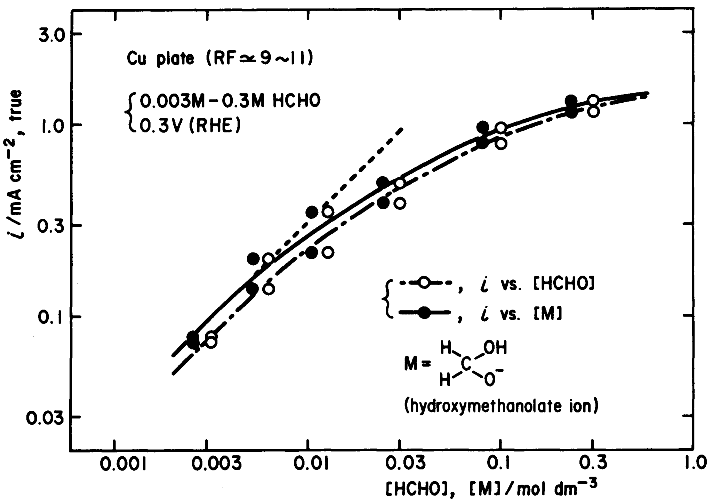

Fig. 11. Anodic current density *i* *vs.* formaldehyde (open circles) and hydroxymethanolate ion (filled circles) concentration observed on Cu plates in 1 M NaOH at 303 K.

Table 1. Equilibrium constant in the system NaOH-HCHO at room temperature

[NaOH]/M	pH	pH[a)]	*K*/M
0.016	12.23	12.20	5.0
0.035	12.52	12.46	4.8
0.096	12.90	12.78	4.4
0.298	13.33	13.02	(7.1)
			Av. 4.7

a) Values obtained in the solutions containing HCHO equimolar with the amount of NaOH.

before any definite interpretations be made: It is nevertheless likely that the hydroxymethanolate ion is adsorbed on the electrode surface prior to its discharge and the adsorption gradually approaches a full coverage in this high concentration region.

On the basis of the experimental observation mentioned above, the following reaction scheme may be written:[10)]

$$HCHO + H_2O \rightleftharpoons CH_2(OH)_2 \tag{1}$$

$$CH_2(OH)_2 + OH^- \rightleftharpoons HOCH_2O^- + H_2O \tag{2}$$

$$HOCH_2O^- \xrightarrow{\wedge} HCOOH + H(a) + e \tag{3}$$

$$HCOOH + OH^- \longrightarrow HCOO^- + H_2O \tag{4}$$

$$2H(a) \longrightarrow H_2\uparrow \tag{5}$$

where $\xrightarrow{\wedge}$ denotes the rate-determining step. The experimental observations, namely, the first order reaction both in HCHO and OH^- at low concentrations, the Tafel line which supports rate-determining one-electron transfer step, one electron involved in the overall reaction, and the hydrogen evolution along with the electro-oxidation, may well be explained by this mechanism.

Additional Remarks. As mentioned above, HCHO is not completely oxidized on the Cu-based electrodes to CO_2 and H_2O at potentials which are desirable for practical fuel cell operations. Also, these electrodes are not good electrocatalysts for the oxidation of hydrogen and hence the hydrogen intermediate yields as gaseous H_2 by step (5). It may therefore be necessary for a complete HCHO oxidation that the Cu-based electrodes may be combined with other electrocatalysts which have a high catalytic activity for the oxidation of $HCOO^-$ and of the hydrogen intermediate,

$$HCOO^- \longrightarrow CO_2\uparrow + H^+ + e \tag{6}$$

$$H(a) \longrightarrow H^+ + e \tag{7}$$

Amorphous alloys are noteworthy in this purpose because they may be prepared in uniform solid solutions with various compositions.

In previous reports,[11)] we have reported that several Ti-and Zr-based amorphous alloys of group VIII metals are good electrocatalysts for the evolution or ionization of hydrogen (Eq 7), and also they are expected to be highly active for the oxidation of $HCOO^-$ (Eq 6). Thus, some preliminary experiments[12)] indicated that, while the electrocatalytic activity in the $HCOO^-$ electro-oxidation of Ni- and Pt-based amorphous alloys was relatively low, that of Pd-based amorphous alloys was very high. Furthermore, the electrocatalytic activity of the Pd-based electrodes was much more stable than that of the other alloys. It may be interesting to see if HCHO can be completely oxidized to CO_2 and H_2O using composite electrodes contaning Cu and Pd.

Conclusion

Cu metal and Cu-based amorphous alloy electrodes show very high electrocatalytic activity for the anodic

HCHO oxidation and the oxidation current is already significant at potentials around 0.1 V (RHE). The reaction kinetics have the characteristics such that the oxidation rate is approximately first order in HCHO and OH^-, and the Tafel line suggests a reaction mechanism involving a rate-determining one-electron transfer step. The results indicate that the oxidation proceeds *via* $HOCH_2O^-$ intermediate which is formed from HCHO and OH^-. The oxidation is, however, not of complete one to CO_2 and H_2O and hydrogen is evolved along with the electro-oxidation.

The present work is partly supported by Grants-in-Aid for Scientific Research No. 59045007 from the Ministry of Education, Science, and Culture.

References

1) J. O'M. Bockris and H. Wroblowa, *J. Electroanal. Chem.*, **7**, 428 (1964).

2) a) "Hydrocarbon Fuel Cell Technology," ed by B. S. Baker, Academic Press, New York (1965); b) J. O'M. Bockris and S. Srinivasan, "Fuel Cells: Their Electrochemistry," McGraw-Hill, New York (1969); c) "From Electrocatalysis to Fuel Cells," ed by G. Sandstede, Battelle Seattle Research Center and the University of Washington, New York (1976).

3) a) S. G. Meibuhr, *Electrochim. Acta*, **11**, 1301 (1966); b) R. T. Tischer, *ibid.*, **11**, 1309 (1966); c) S. G. Meibuhr, *ibid.*, **11**, 1325 (1966); d) S. G. Meibuhr, *ibid.*, **13**, 1973 (1968).

4) W. R. Wolfe and K. B. Keating, *J. Electrochem. Soc.*, **121**, 1125 (1974).

5) T. Kudo, G. Kawamura, and H. Okamoto, *J. Electrochem. Soc.*, **130**, 1491 (1983).

6) a) M. Enyo, *J. Electroanal. Chem.*, **186**, 155 (1985); b) M. Enyo, *J. Appl. Electrochem.*, in press; c) K. Machida and M. Enyo, *Chem. Lett.*, **1985**, 75.

7) A. Kawashima and K. Hashimoto, Proc. 4th Int. Conf. on Rapidly Quenched Metals, Sendai, 1982, Abstr. Vol. 2, pp. 1427—1430.

8) A. J. Maeland, L. E. Tanner, and G. G. Libowitz, *J. Less-Common Met.*, **74**, 279 (1980).

9) K. Machida, M. Enyo, K. Kai, and K. Suzuki, *J. Less-Common Met.* **100**, 377 (1984).

10) a) E. Müller and S. Takegami, *Z. Electrochem.* **34**, 704 (1928); b) R. P. Buck and L. R. Griffith, *J. Electrochem. Soc.*, **109**, 1005 (1962); c) M. Saito, *Kinzoku Hyomen Gijutsu (Metal Surface Technology)*, **16**, 300 (1965); d) J. E. A. M. Van Den Meerakker, *J. Appl. Electrochem.*, **11**, 387 (1981).

11) M. Enyo, T. Yamazaki, K. Kai, and K. Suzuki, *Electrochim. Acta*, **28**, 1573 (1983); K. Machida, M. Enyo, I. Toyoshima, K. Miyahara, K. Kai, and K. Suzuki, *Bull. Chem. Soc. Jpn.*, **56**, 3393 (1983); K. Machida and M. Enyo, unpublished data.

12) K. Machida and M. Enyo, to be published.